ISTITUTO NAZIONALE DI FISICA NUCLEARE

Sezione di Perugia

INFN/AE–98/18
7 Luglio 1998

A. Codino:

A NEW READOUT METHOD FOR MEASURING THE TIME OF FLIGHT OF IONIZING PARTICLES

Published by ***SIS–Pubblicazioni***
Laboratori Nazionali di Frascati

INFN–Istituto Nazionale di Fisica Nucleare
Sezione di Perugia

INFN/AE–98/18
7 Luglio 1998

A NEW READOUT METHOD FOR MEASURING THE TIME OF FLIGHT OF IONIZING PARTICLES

Antonio Codino
Dipartimento di Fisica dell'Università di Perugia and INFN, Italy

ABSTRACT

A new method of processing the output signals of preamplifiers connected to silicon strip detectors operated for time–of–flight measurements is described. Pulse pairs coming out from the two arms of a silicon strip telescope are stored in a transient digitizer with a minimum sampling period of 5 ps and software analyzed. This method eliminates both discriminators and time–to–digital converters from the readout system. Using the new technique the time resolution of the telescope, at various thresholds, is determined by software algorithms that reproduce the functions of both amplitude and constant–fraction discriminators.

Measurements of time resolution of the telescope of the new readout system, using electrons from the source ^{90}Sr are reported. At room temperature, the time resolution of the telescope obtained with unoptimized software algorithms of the new technique is 235±55 ps to be compared with that of 160±35 ps resulting from the use of the classical readout method.

Technical limitations of these measurements are discussed.

1. INTRODUCTION

Detectors for time–of–flight (TOF) measurements consist of two arms, positioned at an appropriate distance, where the passage of an ionizing particle is localized and detected. Signals coming out from preamplifiers or photomultiplier tubes usually connected to the TOF detectors, are discriminated and then sent to the inputs of a Time–to–Digital Converter (TDC) to determine the transit time between the two arms of the TOF detector system. In fig.1 are schematically depicted the two most common readout methods employed in physics experiments. The block diagram in fig. 1–a illustrates the first method which uses a leading–edge discriminator in the signal processing chain. The preamplifier output signal bifurcates in a first chain composed of a shaper and an Analog–to–Digital Converter (ADC) that measures the pulse amplitude and, in a second chain composed of a leading–edge discriminator and a TDC measuring the time interval between the start and the stop signals. The start signal is delivered by a trigger detector ignored in the figure. The measurement of the pulse amplitude is necessary to make time–walk

corrections. These corrections may improve the uncorrected time resolution of a telescope depending on the discriminator threshold (see, for example, fig. 11 of reference [1]).

The second readout method shown in fig. 1–b uses a constant–fraction discriminator which performs time–walk corrections *in situ* avoiding devices for measuring pulse amplitude. The invention and operation of constant–fraction discriminators [2–5] took place 3 decades ago in the attempt to improve the timing accuracy of scintillator counters connected to amplitude discriminators.

Nearly all discriminators presently employed in Nuclear and Cosmic Ray Physics experiments for time–of–flight measurements fall into one of the following categories:

(1) leading–edge discriminators (also called amplitude discriminators);
(2) constant–fraction (CF) discriminators;
(3) extrapolating leading–edge discriminators;
(4) amplitude and rise–time compensated (ARC) discriminators.

Amplitude and constant–fraction discriminators reach the optimum time resolution if the variations of both pulse profiles and rise times are modest. When these 2 parameters suffer large excursions as those occurring in large volume solid state detectors, the use of ARC discriminators might improve the time resolution. The design, construction and operation of ARC discriminators were first reported in 1972 [6,7]. A variant of the classical extrapolating leading–edge discriminators has been recently constructed [8].

Some important aspects of the state of art of electronic devices for reading TOF detector systems are marked in an interesting review article appeared in 1975 [9], after the advent of CF and ARC discriminators. Comparing the old to the recent, analogous instrumentation it seems that no significant progress has occurred in the signal processing chains of fig.1 since two decades. Thus, readout techniques for time–of–flight detectors has not yet benefited from the exceptional development of microelectronics and computing power occurred in the same epoch.

The readout methods mentioned above preassume and operate the destruction of pulse pairs from which the transit time is ultimately extracted. The new readout technique described here stores on an electronic device the two pulse profiles delivered by the detectors forming the 2 arms of the TOF system.

The expected fundamental advantage of this technique is a superior elaboration of the properties of the pulse pairs that might ultimately lead to an unprecedented time resolution.

The perimeter of the work described in this paper is delimited in the following. In Section 2 the silicon telescope and electronic devices utilized in these measurements are described. In Section 3 the parameters affecting the time resolution of the silicon telescope are introduced. The synchronization procedures of pulse pairs relevant to this readout technique are described in Section 4. The results are discussed in Section 5 and various implications of these measurements are given in Section 6.

The major motivation of this set of measurements is to demonstrate that this new readout technique applied to a silicon strip telescope reaches a time resolution comparable to that of classical readout techniques. Neither the ultimate time resolution achievable in various detector configurations nor new software algorithms appropriate for this readout method are investigated here. Thus, the reported measurements have been only taken at room temperature and not at -55^{0}C where the time resolution of the telescope determined by the use of the CF discriminators improves approximately by a factor of 2 reaching the value of 61±7 ps [10] compared to that of

about 120 ps obtained at 20°C [11,12]. It is likely that a comparable improvement of the time resolution at -55°C is also expected by using the new readout technique.

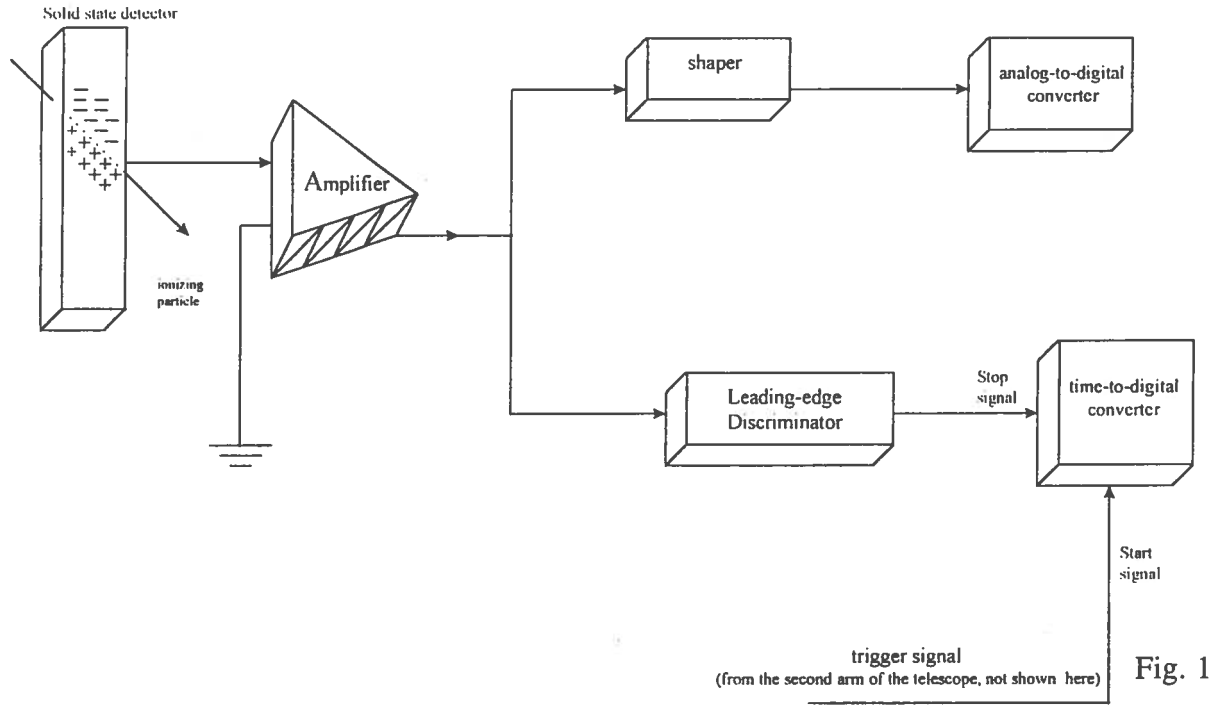

Fig. 1a

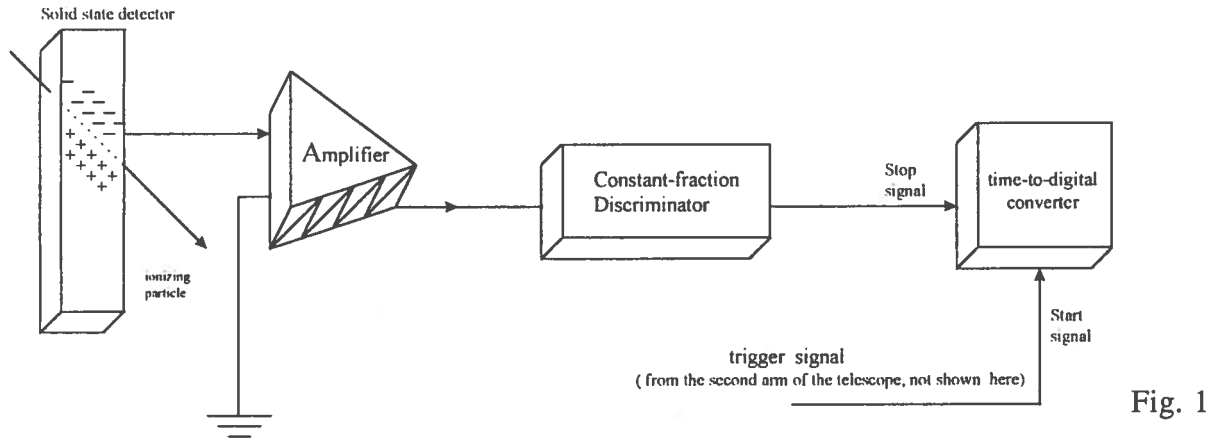

Fig. 1b

Fig. 1 – Block diagrams of the 2 most common methods for processing output signals delivered by detectors used for time–of flight measurements.

2. INSTRUMENT DESCRIPTION AND CHARACTERISTICS

The instrument utilized in these measurements, is formed by one arm of the upgraded version of the COSIDE telescope [10]. The instrument, shown in fig. 2 consists of two orthogonal silicon strip detectors 20 mm long and 2 mm wide defining a useful, sensitive surface of 2x2 mm^2. The signals from each strip are read by a preamplifier and successively by an amplifier. The amplifier output signal is sent to the digital oscilloscope Tektronix SCD1000. This oscilloscope acts as a transient recorder or waveform digitizer with a minimum sampling

period of 5 ps and an input bandwidth of 1 GHz. The two pulses stored in the oscilloscope are read by a program written in LabView 2 language and then transferred to a computer.

The 2 strip detectors are parts of 2 silicon chips, 300 μm thick, of planar dimension of 2×2 cm^2 (300 nm metallization thickness) manufactured by the Micron Semiconductor srl Sussex, England. The chips are segmented in 10 equal detectors of dimensions $0.2\times2\times0.03$ cm^3. Each detector has a capacitance of 15 pF. The detectors of two adjacent chips form an x–y array of 100 TOF elements; however in the measurements reported in this paper only 2 detectors (or elements) are utilized, as shown in fig.2.

The preamplifier [13] consists of two bipolar transistor stages in a current–shunt feedback loop. These transistors (Philips BFQ67) are characterized by a transition frequency (f_T) of 7.5 GHz. An insertion amplifier is connected to the preamplifier output to raise the signal amplitude by a factor of about 60. The insertion amplifier is a two–stages voltage amplifier with a bandwidth of 320 MHz and input and output impedances of 50 Ω.

The profile of the amplifier output signal is interpolated and stored in the digital oscilloscope. It is represented by the coordinate pairs, t_n and $V(t_n)$, where t_n is the time, $V(t_n)$ is the amplitude at the time t_n and n is the n–th interpolation point. The total number of points, N, used for the interpolation is constant and equal to 1024. The sampling step, defined by the time difference, $t_{n+1}-t_n$, is constant in a given set of measurements.

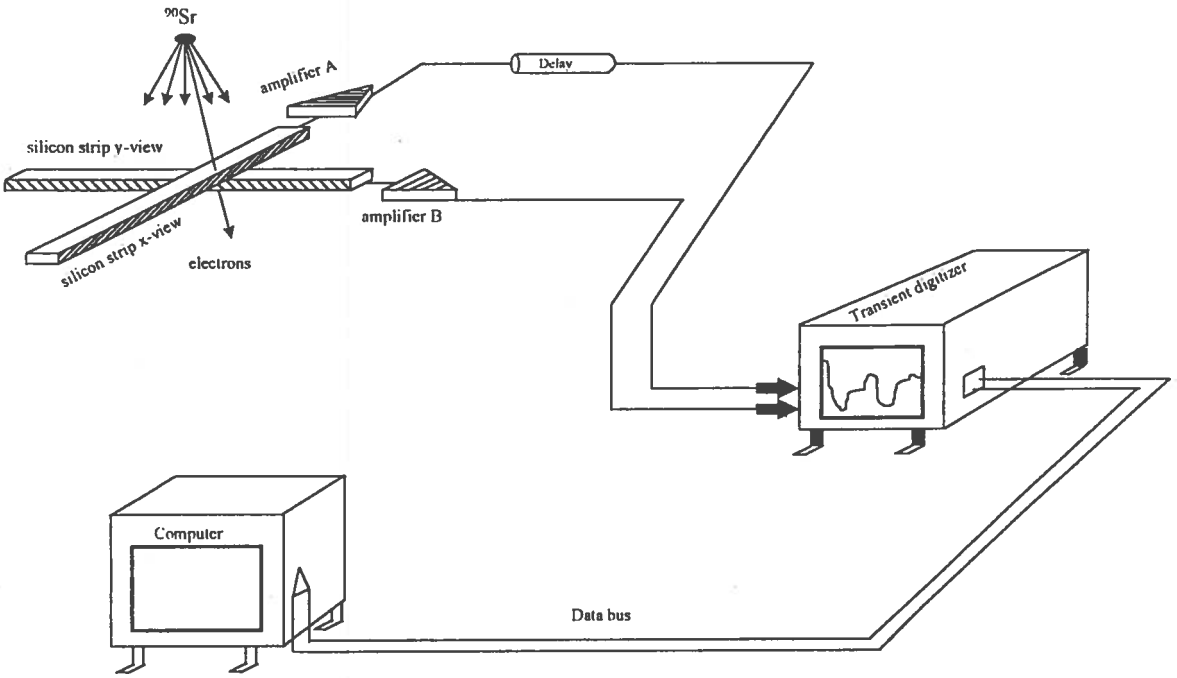

Fig. 2 – Illustration of the experimental layout utilized in the present measurement of the time resolution of time–of–flight detectors. The telescope consists of a pair of silicon strip detectors, current preamplifiers, a transient digitizer and a computer. Electrons from the source ^{90}Sr impinge on silicon strip detectors activating the signal processing chains. The shielding box containing the telescope is not shown in this figure.

The three sets of measurements discussed in Section 5 have sampling steps of 55, 98 and 195 ps. In these conditions, the maximum useful time intervals of the transient digitizer for storing two pulse profiles, D_{max}, given by $N\times(t_{n+1}-t_n)$ are 56, 100 and 200 ns, respectively. Because of these instrumental characteristics, the profiles of pulse pairs coming from the two arms of the telescope can be completely stored in the transient digitizer only if the total width of the first and second pulse together and their delay do not exceed D_{max}. The rise time and fall time distributions of the amplifier output pulses are shown in fig. 3–a and 3–b. Note that rise and fall times may significantly differ in different amplifiers because of the unequal characteristics of the electronic components. These data, collected with the experimental setup shown in fig. 2, indicate that the parameter D_{max} of the oscilloscope is adequate. A typical pulse pair stored in the transient digitizer is shown in fig.4.

For subsequent convenience some basic and critical characteristics of the telescope regarding pulse amplitude distributions and signal shapes at the amplifier output are given. Pulse amplitudes induced by electrons emitted from the source ^{90}Sr and penetrating both silicon strips of the telescope follow the typical Landau distributions with average peak positions of about 120 mV for both strips (see also, for example, figures 2–a and 2–b of the ref. 12). Signal profiles at the amplifier output may be classified in 3 categories depending on the geometrical patterns which have been arbitrarily labelled as: (1) double exponential, (2) trapezoidal and (3) triangular. Examples of these geometrical patterns are displayed in fig. 5. The fractions of these 3 pulse populations are 0.427 (double exponential), 0.330 (trapezoidal) and 0.247 (triangular). These fractions result from the study of a sample of 300 pulse profiles acquired with the oscilloscope Tektronix SCD1000.

3. DOMINANT FACTORS OF THE TIME RESOLUTION

For the correct interpretation of the experimental results given in the subsequent Sections 4 and 5, the following definitions are necessary.

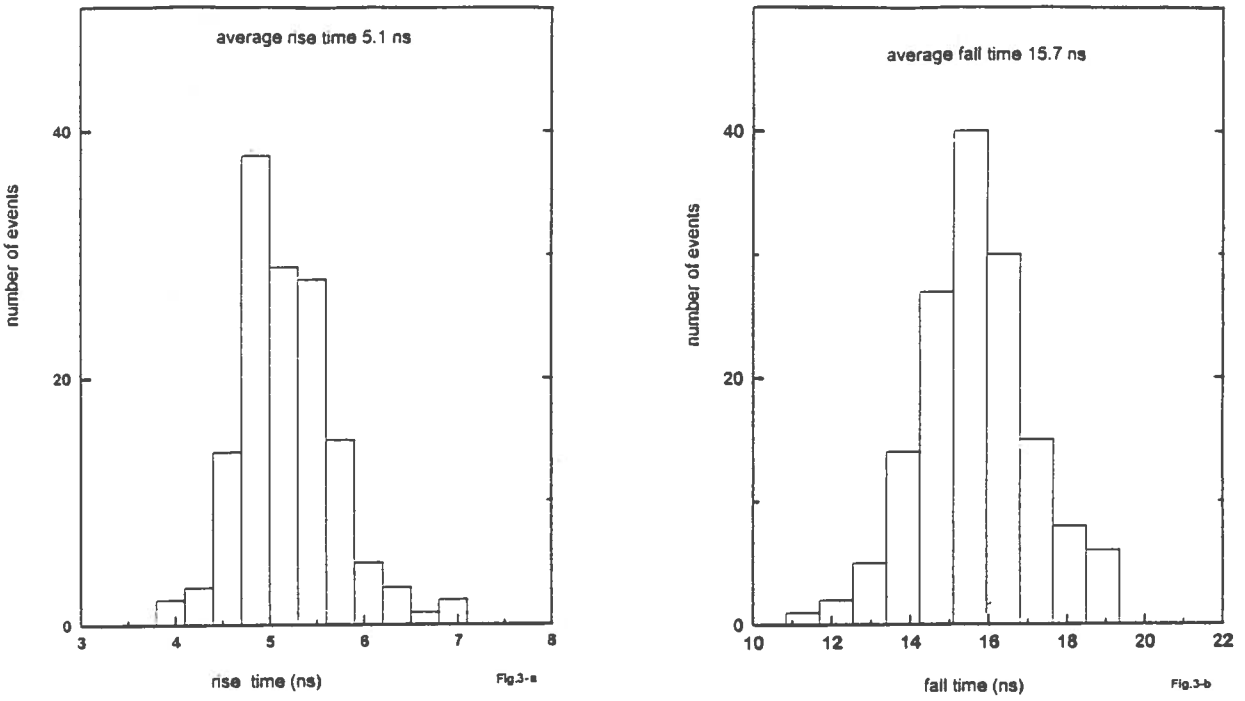

Fig. 3 – Rise time (fig. 3–a) and fall time (3–b) distributions of pulses of a COSIDE preamplifier. The total pulse width is centered at about 20 ns and does not exceed 25 ns.

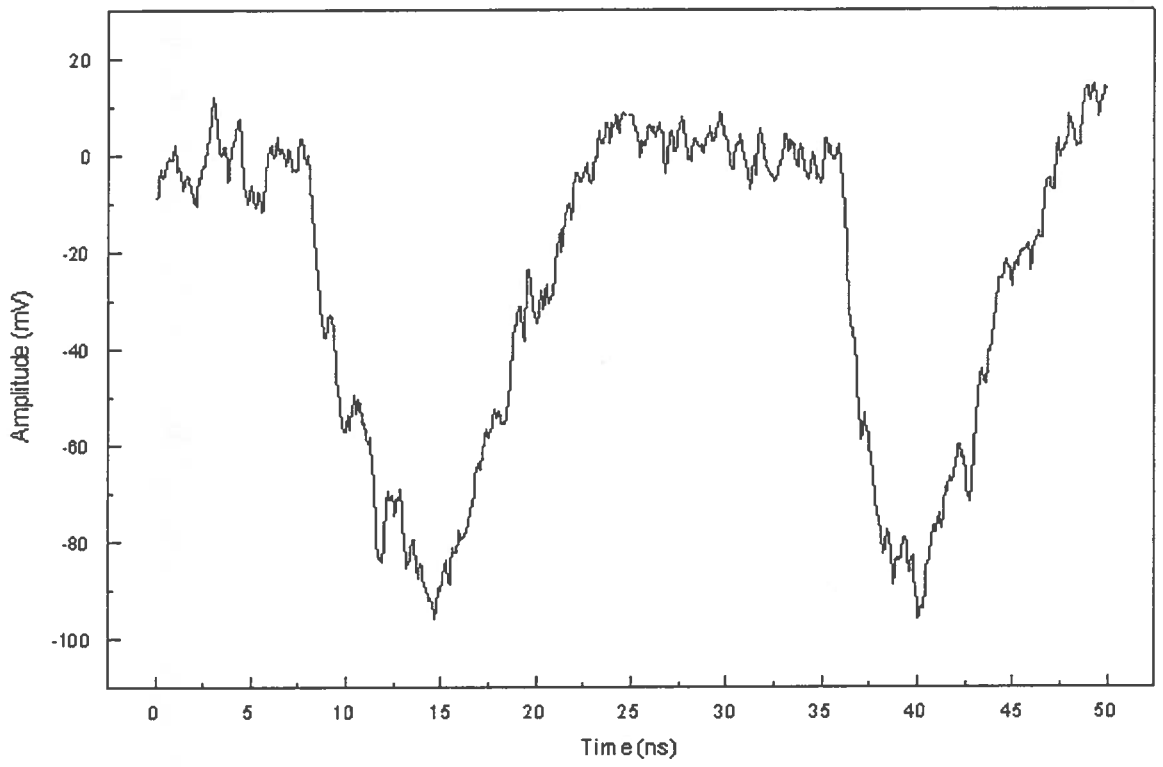

Fig. 4 – Signal profiles of a pulse pair delivered by two COSIDE amplifiers stored with the transient digitizer with a sampling step of 55 ps. These signals are generated by electrons from the ^{90}Sr source that penetrate both the hodoscopes of the instrument.

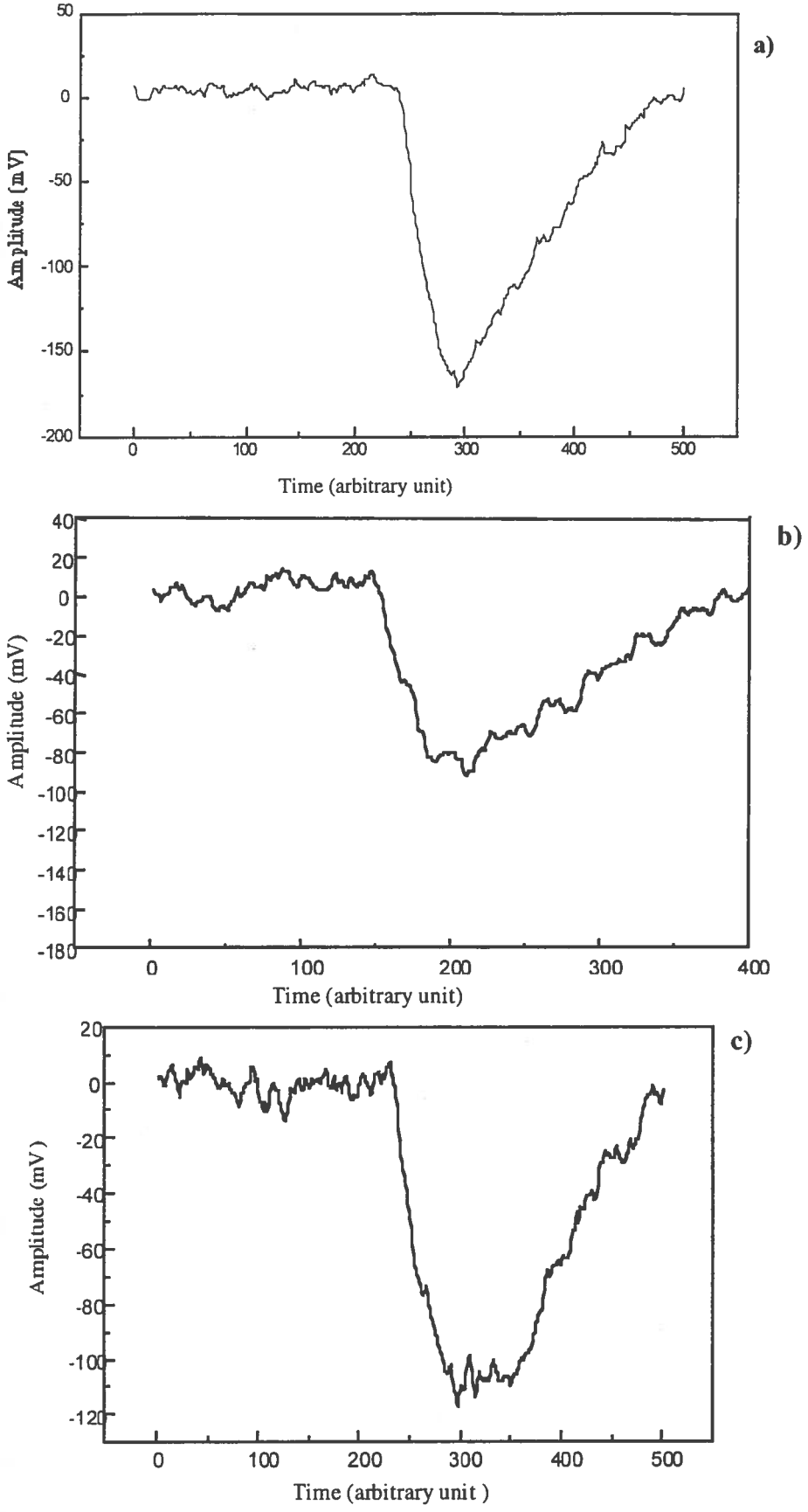

Fig. 5 – Signal shapes at the preamplifier output stored with the transient digitizer. The pulse populations are classified according to the signal profiles: triangular (fig. 5–a), double exponential (fig. 5–b) and trapezoidal (fig. 5–c).

The time interval elapsed in the traversal of the first and second arm of the telescope, T, shown in fig. 2, may be split into 4 contributions:

$$T = T_Z + T_D + T_L + T_C \tag{1}$$

where T_Z is the signal propagation time between the impact point on the strip and the preamplifier input, T_D is the delay introduced by the coaxial cable connecting the amplifier output to the input of the transient digitizer, T_L is the time taken by the leading edge of the pulse to reach the threshold starting from the baseline level, and finally T_C is the transit time of the ionizing particle across the TOF arms. The time resolution, σ_T, is the standard deviations of the distribution of the T. This time resolution has been subdivided into the 4 components σ_Z, σ_D, σ_L and σ_C corresponding, respectively, to the standard deviations of the distributions of T_Z, T_D, T_L, T_C defined above. This subdivision is approximately correct if no significant correlations among the 4 time intervals are present. Following this approximation, appropriate for the instrument shown in figure 2, these 4 time spreads may be added in quadrature as follows:

$$\sigma_T = \left(\sigma_Z^2 + \sigma_D^2 + \sigma_L^2 + \sigma_C^2\right)^{1/2} \tag{2}$$

The parameter σ_Z is calculated to be less than 23 ps for the sensitive cross area of 2 mm^2 of the telescope. In our experimental conditions the quantity σ_D results minor than 10 ps. For relativistic electrons, crossing the average distance of 650 μm between the 2 detector planes of the telescope, T_C is 2.5 ps. As a result, the related time spread for electrons from the ^{90}Sr source σ_C is limited to a few times the value of T_C.

If the silicon telescope is disconnected fron the preamplifier and replaced by an electronic pulser, the global time spread produced by the preamplifier, the waveform digitizer and the procedures adopted for the data analysis can be determined. This determination verifies the calculation on the values and plausible ranges of σ_Z, σ_D and σ_C given above. In this particular measurement the oscilloscope, Tektronix SDC1000 has been replaced by the Tektronix TDS684B, which has two independent acquisition channels but a longer sampling step of 200 ps (the minimum value). Consequently, the electronic noise of one pulse does not interphere with the other. The resulting time spread has a standard deviation less than 15 ps which is compatible with the estimates given above and with similar measurements [14].

Because the measured time resolution of the telescope exceeds 200 ps, the time spreads σ_Z, σ_D and σ_C are totally negligible. From these estimates it results that the time resolution is dominated by the term σ_L which reflects the fluctuations of the electronic noise in the baseline and those of the 2 geometrical patterns of the pulse profiles at the preamplifier outputs.

4. PULSE PAIR SYNCHRONIZATION AND THRESHOLD POSITIONING

In the following discussion regarding the definition of the synchronization of pulse pairs only triangular pulses are considered. Double exponential or trapezoidal profiles or any other profile in the form $V(t_n)$ might be used as well. Triangular profiles are preferred to others because of their simplicity consisting only of 3 straight line segments.

A minimum of 2 pulses is necessary to measure the time interval T given by equation (1). It is assumed in this work that this minimum constitutes the basis for the determination of T. This fundamental assumption is retained in this work although solid state detectors can be employed with tangible advantages in multiple measurements of time of flight involving more

than 2 pulses as demonstrated elsewhere [10]. The 2 pulse profiles are represented by the data sets $V_1(t_n)$ and $V_2(t_{n+m})$ with n and m in the ranges $1 \leq n \leq N_1$ and $N_1 \leq m \leq N_2$ being N_1 and N_2 the number of interpolation points of the first and second pulse, respectively. In order to measure T, pulse pairs must be synchronized. The synchronization defines a time reference where the time of flight is measured. The synchronization is the determination of the time interval between the first and second pulse whenever they are generated in the same experimental conditions. For instance, these conditions may be those of relativistic particles (or any particles with known velocity) traversing the telescope with normal incidence. The procedures for pulse synchronization described below are referred to as baseline, amplitude and barycentric synchronizations. Note that real, physical discriminators in the classical readout chain, regardless the principle of operation, silently accomplish a form of pulse synchronization.

Ideally, a simple method for pulse synchronization is that of taking the 2 instants when the leading edges of the 2 pulses deviate from the noise level of the baseline (baseline synchronization). Consider a pair of triangular profiles as displayed in figure 6–a. These pulses are regarded as ideal because their patterns are noiseless both in the baseline and in the full profiles. An estimator of the time interval T, defined by equation (1), is the time difference, $T_{\alpha\beta}$, between the initial points T_α and T_β along the time axis (see fig. 6–a) $T_{\alpha\beta} = T_\beta - T_\alpha$. The presence of electronic noise in the baseline is a fundamental yet undesirable aspect of the instrument in fig. 2 and alters the ideal profiles. Thus, the time difference $T_{\alpha\beta}$ turns out to be a bad estimator of T. In our experimental conditions the instants T_α and T_β are not measurable with useful accuracy.

Amplitude discriminators in the classical readout chain would measure the time of flight T_A (see fig. 6–a). Generally, $T_{\alpha\beta}$ differs from T_A and both T_A and $T_{\alpha\beta}$ differ from T.

A more adequate procedure for pulse synchronization is the setting of a threshold close to the electronic noise level of the baseline in such a way that it cuts spurious signals and accepts genuine signals.

Using this procedure (that we call amplitude synchronization) the second pulse is anticipated along the time axis by a suitable amount in such a way that both leading edges of the 2 pulses traverse the threshold I of –5 mV in the same instant denoted by t_H in the time axis of fig. 6–b. This operation accomplished at software level by a time translation is called amplitude synchronization. In the approximation and assumptions mentioned above the two pulse profiles are regarded as synchronous at the time $t = t_H$. A second threshold denoted by A_{II} (indicated in fig. 6–a) is used to determine the time interval T, defined by the equation (1), with an algorithm equal to that of the classical readout method using amplitude discriminators (fig. 1–a). When this procedure for pulse synchronization is adopted, the time elapsed between the crossing of the first and the second threshold is a good estimator of T.

Other procedures for pulse synchronization can be conceived as, for example, that using the centers of gravity, τ_1 and τ_2, of the full pulse profiles. In this case:

$$\tau_1 = \frac{\sum_{n=1}^{N_1} t_n V_1(t_n)}{\sum_{n=1}^{N_1} V_1(t_n)} \qquad (3)$$

where N_1 is the number of interpolation points of the first pulse. A similar expression holds for τ_2. With large samples of pulse pairs, the average values of the centres of gravity, $\overline{\tau_1}$

and $\overline{\tau_2}$, can be calculated. The requirement that τ_1 and τ_2 coincide (for instance, with relativistic particles crossing the telescope) makes a pulse pair sample synchronous if a time translation, t_G, given by $t_G = (\overline{\tau_2} - \overline{\tau_1})$ is imposed.

It is likely that t_G and t_H are significantly correlated. In this case, the correlation might give better timing accuracy than that obtained by the amplitude or barycentric synchronizations, separately. In the following, only the amplitude synchronization is employed.

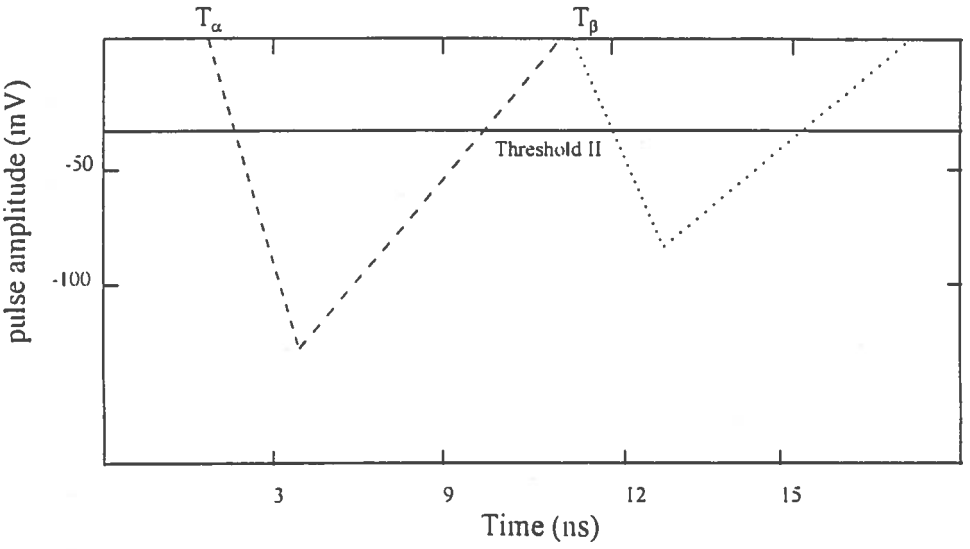

Fig. 6-a

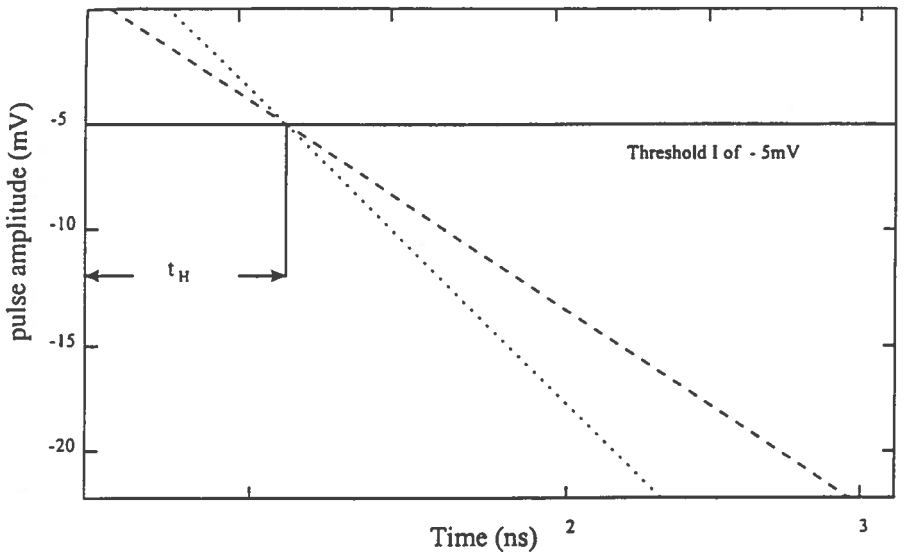

Fig. 6-b

Fig. 6 – Definition of the synchronization of pulse pairs. Two ideal noiseless triangular pulses are shown in fig. 6–a, properly delayed. The time interval measured by the telescope with amplitude discriminators is indicated by T_A.The second pulse is anticipated along the time axis until its leading edge crosses the threshold I, set a –5 mV (fig.6–b). This time translation is necessary in the new readout technique.

5. THE SOFTWARE ALGORITHMS PERFORMING THE FUNCTIONS OF CLASSICAL DISCRIMINATORS

The measurements aiming to reproduce by the new readout technique the basic characteristics of the classical readout methods (illustrated in fig.1) are reported in this Section. The amplitude discriminator (AD) algorithm performs, at software level, (as opposed to physical discriminators which perform at hardware level) the function of the amplitude discriminator in the signal processing chain shown in the figure 1–a. This function is defined in the previous section by using 2 thresholds. The pulse pair from which the time resolution is extracted, is synchronized at the threshold of –5 mV as discussed earlier.

The resulting time resolution versus threshold is shown in figure 7 for a sampling step of 98 ps. As expected, it improves as the software threshold A_{II} approaches the baseline level. At the lowest (absolute) value of 20 mV attains the time resolution of 340±50 ps.

As expected, when slew–rate corrections are applied to these uncorrected data, an improved time resolution is observed, as shown by the data points in the same fig. 7. The expression for the classical algorithm making slew–rate corrections is the following one:

$$\delta t = w\left(\frac{1}{\sqrt{Q_1}} - \frac{1}{\sqrt{Q_2}}\right) \tag{4}$$

where δt is the time correction, Q_1 is the charge of the first pulse, Q_2 that of the second pulse and w is an appropriate constant. The correction entailed in equation (4) is usually applied to scintillator–photomultiplier counters .

The outcome of this algorithm applied to the raw data is shown in fig. 7 (solid dots).

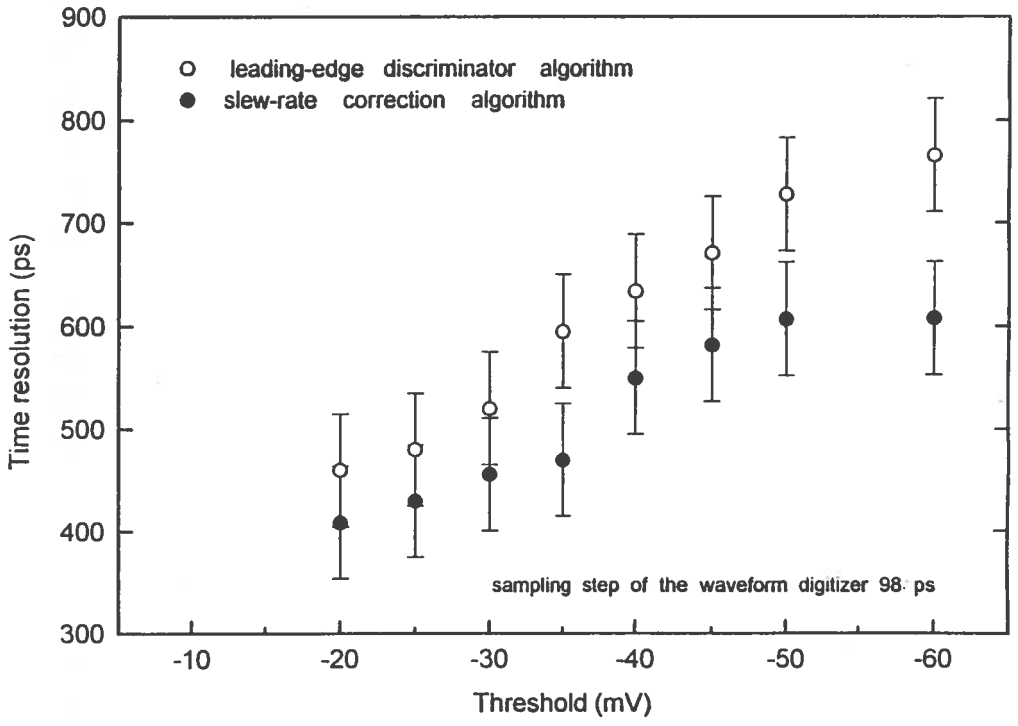

Fig. 7 – Time resolution versus discriminator threshold determined by an algorithm performing the function of the leading–edge discriminator.

The constant–fraction discriminator (CFD) algorithm performs, at software level, the function of constant–fraction discriminators in the signal processing chain shown in figure 1–b. In this case, a constant fraction of the maximum amplitude of the preamplifier output signal is taken for elaboration. The amplitude of the original pulse profile is reduced by a suitable constant fraction, then delayed and inverted. The resulting pulse is summed to the original one yielding a final signal that traverses the baseline after a time interval nearly independent of the amplitude.

In fig. 8 is shown the time resolution as a function of the fraction of the signal amplitude utilized for the elaboration of the CFD algorithm. The sampling step of these measurements is 195 ps.

In fig. 9 is shown the time resolution versus threshold obtained with the CFD algorithm with an optimum constant fraction of the signal amplitude of 30 %. For comparison, in the same figure is given the time resolution obtained with the LA algorithm.

The dependence of the time resolution of the telescope on the duration of the sampling step for the CFD algorithm is displayed in fig. 10. Contrary to what might have been expected from qualitative arguments, very short sampling steps (e.g. 55 ps) do not straightforwardly yield a better time resolution. The unobserved improvement in the time resolution for very short sampling steps might be ascribed to the electronic noise in the baseline which induces fluctuations in the leading edge of current pulses larger than those with longer sampling steps.

The electronic noise in the baseline is the total noise at the amplifier output in the absence of any input signal. This noise has to be distinguished from that present on the leading edge of the pulse crossing the discriminator threshold. While in the classical readout chains (see fig. 1) the noise level at discriminator threshold is important, in this readout technique both the noise in the baseline and that at threshold are crucial. Measurements of these two noise levels in silicon detectors have been previoulsy reported [12].

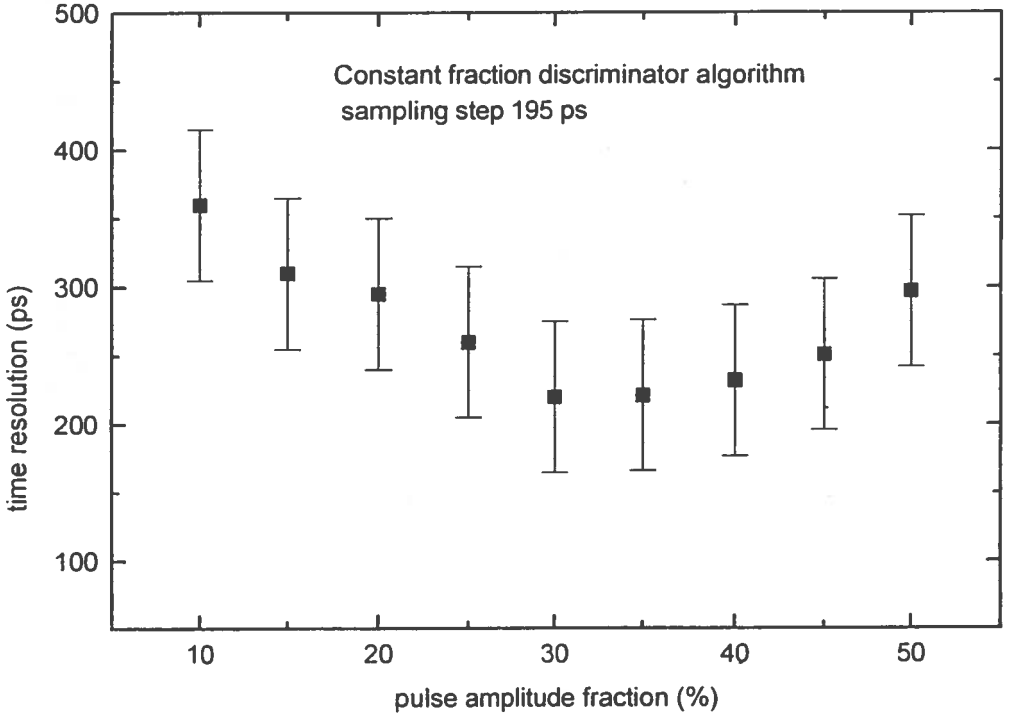

Fig. 8 – Time resolution versus fraction of the pulse amplitude utilized in the algorithm performing the function of a constant–fraction discriminator.

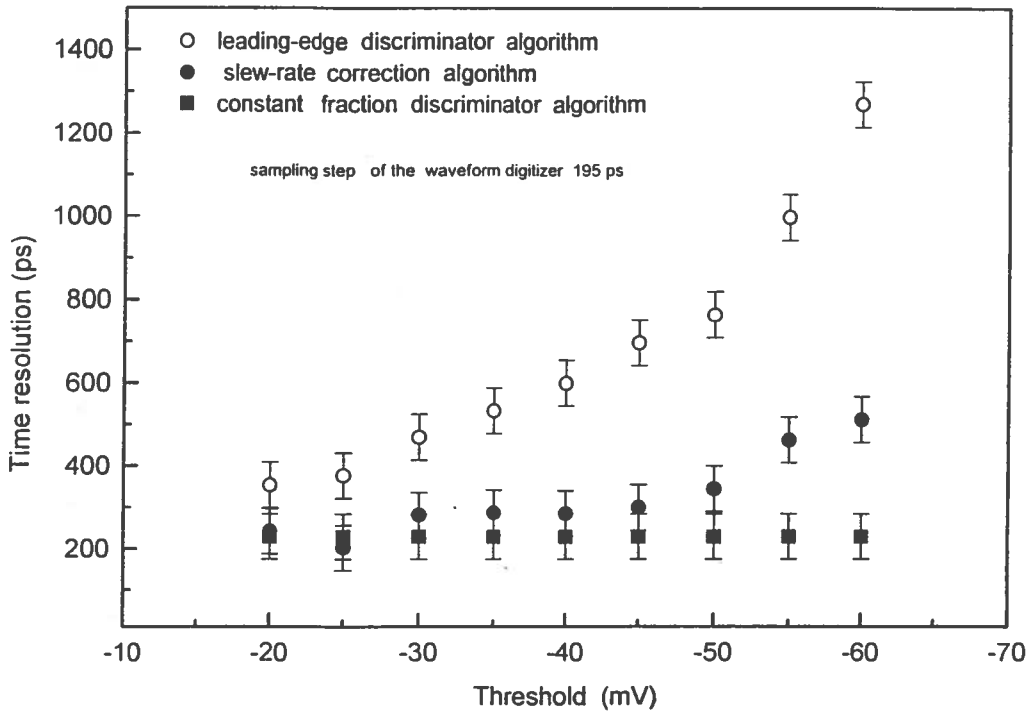

Fig. 9 – Time resolution versus threshold determined by the CFD algorithm with the constant fraction of 30% of the preamplifier output signal. For comparison, the LA algorithms applied to the same data, with and without slew–rate corrections, are shown. The sampling step of these data is 195 ps.

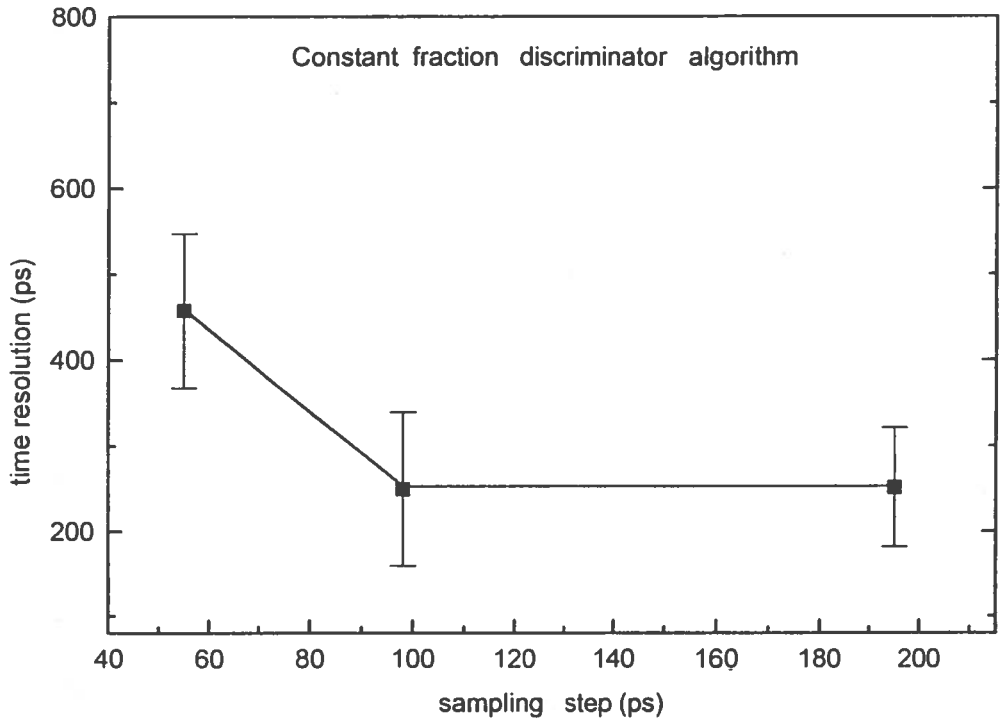

Fig. 10 – Time resolution obtained with the constant–fraction discriminator algorithm versus sampling step of the transient digitizer for the 3 different steps of 55, 98 and 195 ps.

6. CONCLUSIONS AND FURTHER STUDIES OF THE READOUT TECHNIQUE

A silicon strip telescope has been operated at a room temperature of about 20^0C to demonstrate the feasibility of a new readout technique for TOF measurements without using discriminators and TDCs. The results reported in the previous Section indicate that the new readout technique may be applied to solid state detectors for TOF measurements. In fact, the time resolution of the telescope measured with electronic devices of the classical readout systems (amplitude and constant–fraction discriminators connected to TDCs) have been reobtained using software algorithms applied to the pulse profiles stored in the transient digitizer. The reported measurements support the application of this readout technique to the LATIN experiment [10,15,16] that utilizes gallium arsenide strip detectors for time–of–flight measurements.

The use of the single input channel of the digital oscilloscope Tektronix SCD1000 for storing both pulses of the telescope is the major limitation of these measurements. In this condition, the electronic noise sources of the 2 separate readout channels at the amplifier outputs add together. In particular, the tail of the first pulse may disturb the leading edge of the second pulse. This undesired circumstance spoils the time resolution and makes the baseline synchronization mentioned in Section 4, not practical.

The use of this readout technique in the LATIN experiment demands the construction of a dedicated electronic circuit, called here the transient recorder, performing the function played by the transient digitizer Tektronics SCD1000 in the experimental setup of fig.2. A transient recorder circuit per channel is mandatory. Presently, a transient recorder for the LATIN experiment [17] is under construction.

The near independence of the time resolution on the sampling step reported in fig.10 may persist at improved time resolutions (for example in the range 30–40 ps) extracted from pulse pair samples with dedicated, new software algorithms. In this case, the optimum period for sampling the pulse profile will not necessarily be the minimum attainable by using the best electronic components presently available. This circumstance facilitates the construction of the transient recorder circuit of the LATIN experiment.

The concept of eliminating discriminators and TDCs from the readout channels is not obvious. For example, in the design of important future experiments such as ALICE [18], where the construction of 170,000 readout channels for time–of–flight spark chambers is foreseen [19], the classical readout method is still contemplated.

ACKNOWLEDGMENTS

I am indebted with the Tektronix company, and in particular with Franco Chiusa from Milan (Italy) who consented, for one day, the use of the digital oscilloscope TDS684B with an input bandwidth of 1 GHz making possible some measurements described in this paper.

REFERENCES

[1] A. Codino et al. Nucl. Instr. and Methods, **A 398** (1997), 315–323.

[2] P. Weinzierl, Review Scien. Instr., **27** (1956) 226–229.

[3] W. Gruhle, Nucl. Instr. and Methods, **4** (1959) 112–114.

[4] D.A. Gedecke and W.J. McDonald, Nucl. Instr. and Methods, **58**, 253 (1968) 253–260.

[5] J.P. Fouan and J.P.Passerieux, Nucl. Instr. and Methods, **62** (1968) 327–329.

[6] Z.H. Cho and R.L. Chase, Nucl. Instr. and Methods, **98** (1972) 335–347.

[7] Z.H. Cho and R.L. Chase, Nucl. Instr. and Methods, **102** (1972) 299–304.

[8] A.R. Frolov et al., Nucl. Instr. and Methods, **A 356** (1995) 447–451

[9] F.S. Goulding and B.Harvey, Annual Rev. of Nuclear Science, Vol.**25** (1975) 177–240.

[10] A. Codino, Nuclear Physics B (Proc. Suppl.) **54 B** (1997) 305–310.

[11] A. Codino et al., Nucl. Instr. and Methods, **A 364** (1995), 552–559.

[12] A. Codino et al., Nucl. Instr. and Methods, **A 361** (1995), 216–221.

[13] M. Menichelli et al., Nucl. Instr. and Methods, **A 360** (1995), 177–179.

[14] A. Codino, Nucl. Instr. and Methods, **A 410** (1998), 12–18.

[15] M.T. Brunetti et al., the LATIN experiment (1996), unpublished available on request.

[16] A. Codino, Nuclear Physics (Proc.Suppl.) **61 B**, (1998), 295–300.

[17] M.T. Brunetti et al., Addendum C of the LATIN experiment (1997), unpublished available on request.

[18] ALICE collaboration, Internal Report CERN/LHCC 95–71 and CERN/LHCC 96–32

[19] E. Badura et al., GSI Scientific Report (1994) page 294, Darmstadt, Germany.